Available online at www.sciencedirect.com
ScienceDirect
Geochimica et Cosmochimica Acta 72 (2009) 1415–1426
Geochimica et Cosmochimica Acta
www.elsevier.com/locate/gca

Core formation and the oxidation state of the Earth: Additional constraints from Nb, V and Cr partitioning

Bernard J. Wood [a,*], Jon Wade [b], Matthew R. Kilburn [c]

[a] GEMOC, Department of Earth and Planetary Sciences, Macquarie University, NSW 2109, Australia
[b] Planetary and Space Sciences Research Institute, The Open University, Walton Hall, Milton Keynes MK7 6AA, UK
[c] Centre for Microscopy, Characterisation and Analysis, University of Western Australia, 35 Stirling Highway, Crawley, WA 6009, Australia

Received 5 June 2007; accepted in revised form 29 November 2007; available online 13 January 2008

Abstract

We have combined metal–silicate partitioning data from the literature with new experimental results at 1.5–8 GPa and 1480–2000 °C to parameterize the effects of pressure, temperature and composition on the partitioning of V, Cr and Nb between liquid Fe metal (with low S and C content) and silicate melt.

Using information from the steelmaking literature to correct for interactions in the metal phase, we find that, for peridotitic silicate melts, metal–silicate partition coefficients are given by:

$$\log\left[D_{\mathrm{Nb}}^{\mathrm{met/sil}}\right] = 2.5\log\left[D_{\mathrm{Fe}}^{\mathrm{met/sil}}\right] + 1.57 - \frac{11,930}{T} - \frac{114(\pm 43)P}{T} \pm 0.41$$

$$\log\left[D_{\mathrm{V}}^{\mathrm{met/sil}}\right] = 1.5\log\left[D_{\mathrm{Fe}}^{\mathrm{met/sil}}\right] + 0.582 - \frac{6493}{T} - \frac{62(\pm 19)P}{T} \pm 0.08$$

$$\log\left[D_{\mathrm{Cr}}^{\mathrm{met/sil}}\right] = \log\left[D_{\mathrm{Fe}}^{\mathrm{met/sil}}\right] + 0.643 - \frac{4232(\pm 538)}{T} - \frac{22(\pm 13)P}{T}$$

where $D_i^{\mathrm{met/sil}}$ is the partition coefficient for element i. Partitioning of V and Cr is insensitive to silicate melt composition, but Nb shows a considerable compositional effect.

The new data enable us to examine different models of terrestrial accretion and core formation. If we fix the Fe content of the mantle at the current value and use the Ni content of the mantle to estimate pressure of equilibration then temperatures about 1200 °C above the silicate liquidus are required to match vanadium partitioning to the current concentration of V in the mantle. Under these conditions the core concentrations of Si (~15%) and Nb (>60% of Earth's budget) are implausibly high. A more realistic approach is to assume that the metal of accreting planetesimals equilibrated at the base of a deep magma ocean whose temperature was close to the silicate liquidus. As the magma ocean deepened in proportion to the size of the Earth the metal was continuously extracted to the core without further re-equilibration in the lowermost mantle. In this case the V, Cr and Nb contents of core and mantle can easily reproduce the expected values provided the Earth became more oxidized as it accreted (O'Neill H. S. (1991) The origin of the Moon and the early history of the Earth—a chemical model. 2. The Earth *Geochim. Cosmochim. Acta* **55**(4), 1159–1172; Wade J. and Wood B. J. (2005) Core formation and the oxidation state of the Earth. *Earth Planet. Sci. Lett.* **236**, 78–95; Wänke H. and Dreibus G. (1988) Chemical-composition and accretion history of terrestrial planets. *Philos. Trans. Roy. Soc. Lond. A-Math. Phys. Eng. Sci.* **325**(1587), 545–557). Increasing oxidation requires the oxidized Fe content of the mantle to increase from 0.5% to 1.0% to the current value of 6.26% as the Earth grew. This model , with magma ocean thickness corresponding to 35% of mantle depth, reproduces the calculated core–mantle partitioning of Ni, and Co and yields a Si content of the core of approximately 6%, in good agreement with cosmochemical estimates.

* Corresponding author.
E-mail address: bwood@els.mq.edu.au (B.J. Wood).

0016-7037/$ - see front matter © 2008 Elsevier Ltd. All rights reserved.
doi:10.1016/j.gca.2007.11.036

1. INTRODUCTION

The earliest history of the Earth was marked by accretion and core formation within about 30 Myr (Kleine et al., 2002; Yin et al., 2002) and formation of the moon by giant impact approximately 40 Myr after the origin of the solar system (Halliday, 2004). Radiogenic isotopes (Kleine et al., 2002; Yin et al., 2002) provide information on the timing of these events while dynamical modeling yields general insight into the physics of planetary formation (Canup, 2004). More precise information on the conditions of core formation depends, however, on a knowledge of how siderophile elements such as Ni, Co and W partitioned themselves between the core and the mantle as the metal phase segregated.

As the earth accreted and the core segregated, all elements were distributed between the Fe-rich metallic phase and the silicate mantle according to their partition coefficients D_i defined as follows:

$$D_i = \frac{[\mathrm{i}]_{\mathrm{metal}}}{[\mathrm{i}]_{\mathrm{silicate}}} \quad (1)$$

where [i] is the concentration of element I in the phase of interest. Elements with high values of D (siderophile) were strongly depleted in the silicate mantle while those with low D values (lithophile) were concentrated in the mantle. These qualitative observations are placed in context by using the observation that the bulk composition of the Earth has strong affinities with those of chondritic meteorites (Allègre et al., 1995; McDonough and Sun, 1995). Refractory lithophile elements are present in the mantle in approximately chondritic proportions to one another which implies that all refractory elements are present in the bulk Earth (core plus mantle) in approximately chondritic proportions. Table 1 presents estimated core–mantle partition coefficients for a number of refractory elements based on this chondritic reference model. In principle these core–mantle values may be used to estimate conditions of core formation because metal–silicate partitioning depends on pressure, temperature, oxygen fugacity and the compositions of metal and silicate phases. The most obvious dependence is on oxygen fugacity, since transfer of an element (M) of valence n from silicate to metal involves reduction:

$$\mathrm{MO}_{n/2} = \mathrm{M} + \frac{n}{4}\mathrm{O}_2 \quad (2)$$

Table 1
Partition coefficients consistent with core–mantle equilibration

Element	McDonough and Sun (1995); McDonough (2003)	Allègre et al. (1995)	Likely range
D_{V}	1.83		1.5–2.2
D_{Cr}	3.4	2.9	2.5–3.5
D_{Fe}	13.66	13.65	13.65
D_{Co}	23.8	24.7	23–26
D_{Ni}	26.5	24.4	24–27
D_{Nb}	—	—	0–0.8
D_{Si}	0.28	0.34	0.1–0.35

Applying the current concentration of FeO in the mantle of about 8 weight % and of Fe in the core of 80% (Allègre et al., 1995; McDonough and Sun, 1995), reaction (2) yields an apparent oxygen fugacity of core segregation approximately $2\log f\mathrm{O}_2$ units below Fe–FeO (IW) equilibrium. If performed at known oxygen fugacity, the stoichiometry of the redox reaction enables experimental measurements of metal silicate partitioning for element M to be extrapolated to any desired oxygen fugacity conditions. In general, however, calculation of oxygen fugacity requires assumptions about the mixing properties of silicate melt which are not well known. So, an alternative approach discussed by Wade and Wood (2005) was adopted. In this case the dependence on oxygen fugacity may be replaced by a dependence on the FeO/Fe ratio, i.e. on the ratio of oxidized to reduced iron. This may be represented by the equilibrium:

$$\underset{\text{silicate}}{\mathrm{MO}_{n/2}} + \frac{n}{2}\underset{\text{metal}}{\mathrm{Fe}} = \frac{n}{2}\underset{\text{silicate}}{\mathrm{FeO}} + \underset{\text{metal}}{\mathrm{M}} \quad (3)$$

When applying equilibrium (3), the oxygen fugacity need not be explicitly known since it is implicitly defined by the FeO/Fe ratio. In addition to oxygen fugacity, redox and exchange reactions such as (2) and (3) depend on pressure and temperature. Thermodynamic data for metals and oxides measured at one atmosphere pressure provide a good basis for extrapolation of experimentally measured metal–silicate partitioning to the very high temperatures consistent with core segregation in a planet the size of Earth (Wade and Wood, 2005). In contrast to temperature, the effect of pressure is, for most elements, impossible to calculate because the requisite data, the partial molar volumes of elements in metal and silicate phases are not available. In order to estimate the effect of pressure on partition coefficients, therefore, high-pressure metal–silicate partitioning data are essential.

High pressure experimental data have shown that the partition coefficients of some siderophile elements (notably Ni and Co) decrease as pressure increases (Li and Agee, 2001) while others such as Si (Gessmann et al., 2001) become more siderophile at high pressure. In a recent summary of available data (Wade and Wood, 2005) we concluded that Ni, Co, W, P and Ga become less siderophile with increasing pressure, while Si and Mn prefer the metal more strongly as pressure increases. The pressure-effect on vanadium partitioning was found, based on relatively few high-pressure data, to be insignificant. Vanadium partitioning between core and mantle (Table 1) was, however, determined to be sensitive to the temperature and oxygen fugacity conditions of core segregation.

By combining the pressure and temperature dependences of partitioning behaviour for a number of elements one can calculate, for fixed mantle composition, a pressure and temperature at which the core and mantle would, at equilibrium, generate the partition coefficients of Table 1. The result, at the current composition of the mantle, is a pressure of about 40 GPa and temperature of ~3800 K (Gessmann and Rubie, 2000; Chabot and Agee, 2003; Wade and Wood, 2005). The observation that high pressures are needed to explain the Ni and Co concentrations in the mantle led to the 'deep magma ocean' hypothesis which, at its simplest, is interpreted as core–mantle equili-

bration at a single pressure, temperature and mantle composition. In this interpretation (Li and Agee, 1996; Righter and Drake, 1997) droplets of metallic liquid descended through a 700 km deep magma ocean, equilibrating with the silicate liquid as they fell (Rubie et al., 2003). The liquid metal ponded at the base of the magma ocean and subsequently descended in large diapirs to the growing core without further equilibration with the surrounding silicate.

In an earlier paper (Wade and Wood, 2005) we extended the deep magma ocean model by taking account of the fact that since small asteroids and planets such as Mars have cores, the Earth almost certainly had a core when it was a Mars-sized body. The core must, therefore have segregated continuously during accretion with concomitant increases in pressure and temperature as the planet grew. The same kind of model is used to calculate the apparent mean-life of Earth accretion from W-isotope data (Yin et al., 2002; Kleine et al., 2004). In order to develop a physically realistic model of the magma ocean on the growing Earth, Wade and Wood (2005) argued that the base of the magma ocean must have remained at a temperature close to the liquidus of the mantle silicate. This fixed point allows for the strong viscosity contrast between the liquid upper part of the mantle and the solid lower mantle above which the metal would have ponded. Applying this constraint and using experimental data for the refractory elements V, Ni, Co and W, we found that the estimated core–mantle partitioning values could only be matched if the Earth became about 2log-fO_2 units more oxidized as it accreted. This progressive oxidation would be consistent with a magma ocean which averaged about 40% of mantle depth and a mean temperature of core segregation slightly below 3000 K.

The principal uncertainties in the quantification of the deep magma ocean hypothesis derive, of course from uncertainties in the experimental partitioning data. In this context, elements whose partitioning is strongly temperature-dependent, such as V are important. It is also important that other moderately siderophile refractory elements are added to the database in order to test the model more extensively. The aims of the current study are firstly to revisit the pressure dependence of vanadium partitioning since our initial study (Wade and Wood, 2005) was based on few data above 3 GPa for this element. Second, Nb is known to be weakly siderophile (Wade and Wood, 2001) and we wish to determine whether core segregation is consistent with the slight Nb deficit in the silicate Earth (Rudnick et al., 2000). Finally, although its oxidation state is not well-constrained under conditions of metal saturation, chromium is another refractory element which can be applied to estimate conditions of core formation and we have performed experiments at 2.5–8 GPa in order to be able to parameterise its partitioning behaviour.

2. EXPERIMENTAL METHODS

We conducted liquid metal–liquid silicate partitioning experiments at low (1.5–2.5 GPa) and high (8 GPa) pressures for a range of siderophile trace elements under conditions where the metal contains between 0 and 9.5% Si. The metallic part of the charge consisted of Fe, $Fe_{83}Si_{17}$and FeS mixed in varying proportions together with about 2% each of Ni, Co and W. By varying the amount of $Fe_{83}Si_{17}$ we were able to vary the oxygen fugacity of the experiment, Si being in metallic form only at very low oxygen fugacity. The silicate part was a synthetic basalt (Kilburn and Wood, 1997) to which about 1% each of the oxides of V, Cr, Mn, Ga and Ta were added. Approximately equal proportions of metal and silicate starting materials were intimately ground together under acetone.

All 2.5 GPa experiments were performed in an 0.5″ piston–cylinder apparatus using polycrystalline MgO capsules (Kilburn and Wood, 1997). The pressure cell consisted of concentric sleeves of pressed $BaCO_3$ (outer), silica glass (inner) and graphite furnace. A single experiment (0710) was conducted at 1.5 GPa in an Fe metal capsule with a tight-fitting lid. In this case a Na-rich starting silicate was used to ensure that the silicate was molten at 1753 K and 0.15% V (as oxide) was added to the charge. Temperature control in all experiments was via a W/Re thermocouple, placed directly above the capsule and the experiment was quenched by turning off the power to the furnace. Experiments at 2.5 GPa were held at temperature for 45 min while the 1.5 GPa/1753 K experiment lasted 35 min (The reason for the shorter duration is that the S-rich liquid escapes from the capsule by solution-reprecipitation in longer experiments). Based on previous studies (Thibault and Walter, 1995; Chabot and Agee, 2003) experiments of 5 min duration are long enough for approach to equilibrium between liquid metal and liquid silicate.

Experiments at 8 GPa were performed in a Walker-type multi-anvil apparatus (Walker et al., 1990) using cast MgO octahedra with fins to support the carbide anvils. The capsule was made of polycrystalline MgO and the furnace was a $LaCrO_3$ cylinder of 5 mm O/D and 3 mm ID. Temperature control was through a W/Re thermocouple in contact with the top of the capsule. Experiment duration was 5 min.

Experimental samples were mounted in epoxy, ground and polished. In most cases, analysis for major and minor elements was performed using a JEOL 8600 electron microprobe using a range of metal, oxide and silicate standards and conditions of 20 kV accelerating voltage with 15 nA beam current. All analyses were made with a 10-μm microprobe spot and results corrected for interferences between Ti, V, Cr and Mn. All microprobe corrections were made using the ϕ-ρ-z approach and a number of well-known standards such as St. John's Island Olivine and KK1 hornblende employed as checks on the calibration. At least 20 analyses were made of both metal and silicate phases to derive the averages and standard deviations shown in Table 2. In one case (experiment 0710) major element analysis was performed using the Cameca SX100 microprobe in the Geochemical Analysis Unit, ARC National Key Centre GEMOC at Macquarie University. Trace element analyses in this case were obtained using a laser ablation ICPMS (LA-ICPMS) system (with 60-μm laser spot) in the Geochemical Analysis Unit and the procedures described in (Norman et al., 2005). Si and Fe were used as internal standards for silicate and metal phases respectively and five analyses each of metal and silicate performed . Experimental data are presented in Table 2.

Table 2
Experimental results

Experiment name	Ala	σ	A2a	σ	A3	σ	MK81	σ	MK84	σ	Bl	σ	B2	σ	b3	σ	cla	σ	c5	σ	101a	σ	103a	σ	710	σ
Tempature (K)	2023		2023		2023		2273		2273		2023		2023		2023		2023		2023		2023		2023		1753	
P	2.5		2.5		2.5		8.0		8.0		2.5		2.5		2.5		2.5		2.5		2.50		2.50		1.5	
Silicate analysis																										
O	39.59	0.51	42.93	0.19	42.99	0.22	41.01	0.34	43.38	0.27	39.11	0.72	40.78	0.64	44.21	0.31	41.63	0.17	46.01	0.09	43.29	—	46.47	—	43.80	
Na	1.39	0.20	1.30	0.08	1.34	0.10	0.47	0.08	0.40	0.08	1.47	0.34	1.56	0.26	0.97	0.17	0.97	0.07	0.70	0.05					4.92	0.82
Mg	16.11	1.49	14.89	1.01	15.99	1.11	20.24	1.53	18.24	0.90	14.02	0.40	16.06	2.00	22.21	1.97	15.92	1.47	18.01	1.24	13.96	1.75	17.13	1.81	0.77	0.02
Al	5.42	0.25	6.65	0.31	6.84	0.36	4.42	0.83	6.06	0.62	4.67	0.46	6.12	0.61	5.00	0.65	5.49	0.35	3.59	0.24	2.69	0.38	3.30	0.35	4.32	0.03
Si	13.90	0.21	18.40	0.19	18.14	0.12	15.41	0.64	18.59	0.19	14.05	0.40	14.81	0.39	18.40	0.14	16.85	0.17	24.33	0.32	15.50	0.46	17.42	0.25	28.82	0.34
S	0.24	0.03	0.28	0.02	2.54	0.19	0.03	0.02	0.04	0.02	0.20	0.04	0.25	0.03	1.18	0.15	0.10	0.02	1.22	0.08	0.19	0.02	0.23	0.03	0.04	0.00
K	0.20	0.03	0.22	0.01	0.24	0.02	0.09	0.02	0.07	0.02	0.22	0.04	0.26	0.04	0.14	0.02	0.13	0.01	0.11	0.01	0.65	0.09	0.49	0.06	—	—
Ca	8.33	0.85	8.26	0.44	8.29	0.51	5.01	0.72	5.05	0.32	9.20	0.93	9.43	1.17	5.90	0.97	6.24	0.54	4.43	0.36	12.14	1.20	9.65	1.03	0.02	0.01
Ti	1.83	0.17	1.76	0.08	1.61	0.08	1.10	0.14	1.20	0.07	1.91	0.25	2.04	0.22	1.24	0.15	1.41	0.10	0.89	0.07	0.22	0.07	0.33	0.35	—	—
V	0.52	0.04	0.34	0.01	0.09	0.01	0.81	0.12	0.77	0.05	0.38	0.07	0.63	0.89	0.11	0.01	0.90	0.01	0.08	0.01					0.43	0.01
Cr	0.28	0.04	0.22	0.01	0.11	0.01	0.51	0.10	0.42	0.04	0.14	0.04	0.34	0.07	0.07	0.01	0.61	0.01	0.11	0.01	0.07	0.02	0.12	0.01	0.21	0.01
Mn	1.87	0.09	1.84	0.03	1.81	0.15	1.73	0.13	1.85	0.08	1.83	0.06	2.06	0.09	1.32	0.06	1.65	0.06	1.23	0.05	1.28	0.05	1.46	0.07		—
Fe	6.91	0.38	0.66	0.01	0.19	0.02	6.75	0.52	2.01	0.15	10.33	0.53	2.66	0.13	0.13	0.01	6.53	0.02	0.31	0.04	5.90	1.35	1.11	0.20	13.10	0.25
Co	—	—	—	—	—	—	0.03	0.01	—	—	0.01	0.00	—	—	—	—	—		—	—	—	—	—	—	—	—
Ni	—	—	—	—	—	—	—	—	—	—	—	—	—	—	—	—	—		—	—	—	—	—	—	0.58(Nb)	0.01
Ga	0.10	0.01	—	—	—	—	0.12	0.03	—	—	0.20	0.02	—	—	—	—	0.09									
Ta	1.43	0.18	1.34	0.07	0.66	0.01	0.75	0.13	0.53	0.08	1.51	0.28	1.60	0.22	0.58	0.08	0.91	0.06	0.43	0.03	—	—	—	—	—	—
W	0.10	0.02	—	—	—		0.05	0.02	—	—	0.33	0.04	—	—	—	—	—		—	—	—	—	—	—	—	—
Silicate total	98.2		99.1		100.8		98.5		98.6		99.6		98.6		101.5		99.4		101.4		95.87		97.73		98.0	
Metal analysis																										
O	—	—	—	—	—	—	0.37	0.00	0.13	0.01	—	—	—	—	—	—	—		—	—	—	—	—	—	0.56	0.68
Si	0.00	0.00	0.76	0.02	7.20	0.30	0.14	0.01	0.93	0.03	—	—	0.01	0.02	5.99	0.14	0.00	0.01	9.50	0.23	—	—	—	—	0.01	0.00
S	2.92	0.58	2.12	0.30	2.53	1.23	3.92	0.67	4.00	0.51	2.32	0.57	2.66	0.65	0.89	0.62	2.92	0.16	1.28	0.87	2.01	1.52	2.17	1.04	2.01	6.15
Ti	—	—	0.01	0.01	0.09	0.04	0.01	0.01	0.02	0.01	—	—	—	—	0.04	0.01	—	0.00	0.03	0.02	—	—	—	—	—	—
V	0.02	0.01	0.87	0.06	1.77	0.16	0.17	0.04	0.61	0.09	0.01	0.01	0.16	0.04	1.59	0.08	0.06	0.02	1.22	0.32	—	—	—	—	0.0156	0.0013
Cr	0.07	0.03	0.86	0.06	1.47	0.13	0.32	0.12	0.83	0.06	0.02	0.01	0.37	0.05	1.27	0.04	0.16	0.02	0.96	0.15	0.04	0.01	0.68	0.06	0.0296	0.0004
Mn	0.04	0.02	0.45	0.05	2.21	1.22	0.24	0.06	0.57	0.05	0.02	0.01	0.15	0.02	1.08	0.67	0.03	0.17	0.45	0.34	—	—	0.25	0.07	—	—
Fe	86.02	0.54	86.75	0.72	74.99	2.18	83.59	0.75	82.63	0.62	87.22	0.49	85.65	1.84	78.45	1.12	84.94	0.45	77.79	1.59	87.73	1.55	89.11	1.13	97.00	7.07
Co	2.24	0.03	1.88	0.03	1.99	0.06	2.05	0.02	1.88	0.02	2.27	0.05	1.81	0.05	2.20	0.05	2.23	0.02	1.97	0.05	0.51	0.02	0.45	0.01	—	—
Ni	2.22	0.06	1.89	0.03	1.85	0.09	2.10	0.03	1.96	0.03	2.26	0.04	1.79	0.05	2.17	0.08	2.26	0.02	1.98	0.06	5.89	0.13	4.42	0.10	—	—
Ga	1.50	0.03	1.57	0.05	1.86	0.08	1.31	0.05	1.41	0.04	1.39	0.06	1.38	0.05	1.68	0.04	1.55	0.02	1.52	0.04	—	—	—	—	—	—
Mo	1.89	0.09	1.45	0.04	1.59	0.12	1.72	0.11	1.72	0.15	1.78	0.05	1.49	0.07	1.65	0.12	2.06	0.06	1.61	0.07	—	—	—	—	—	—
Ta	—	—	—	—	0.74	0.28	0.01	0.01	0.03	0.01	—	—	0.01	0.01	0.65	0.21	—	—	0.08	0.04	—	—	—	—	(0.00085 Nb)	0.0003
W	1.45	0.05	1.50	0.05	1.63	0.10	1.37	0.05	1.35	0.04	1.53	0.07	1.44	0.09	1.55	0.06	1.59	0.04	1.27	0.04	—	—	—	—	—	—
Metal sum	98.35		100.11		99.91		97.31		98.07		98.82		96.92		99.18		97.81		99.64		96.17		97.07		99.60	
γ activity coeff.																								Nb	0.06	
Fe	1.00		1.00		0.80		1.01		1.00		1.00		1.01		0.87		1.01		1.00		1.00		1.01		1.01	
V	0.08		0.10		0.16		0.08		0.10		0.08		0.08		0.17		0.08		0.10		0.08		0.09		0.03	
Cr	0.82		0.88		0.73		0.75		0.81		0.84		0.85		0.82		0.82		0.91		0.91		0.92		0.76	

2.1. Corrections for solutes in alloys

Because trace elements in metal alloys interact strongly with the major components such as Fe, C, S and Si, it is necessary to correct the partitioning data to a common reference point, in this case the effective value for pure metallic element in the liquid state. To perform these corrections we followed the thermodynamic approach employed by Wade and Wood (2005), which is based on the 'Wagner ε formalism' (Wagner, 1962) This represents the effects of different solutes on one another's thermodynamic properties as follows:

$$\ln \gamma_i = \ln \gamma_i^o + \sum_{j=2}^{N} \varepsilon_i^j x_j \tag{4}$$

In Eq. (4), γ_i is the activity coefficient of solute i in the mixed alloy and γ_i^o is its activity coefficient when it is infinitely dilute in pure liquid Fe under the same conditions of pressure and temperature. The interaction parameters ε_i^j refer to the measured effects of component j on the activity of i in the alloy and are assumed to be linearly dependent on the mole fraction of j, x_j. A large number of experiments have been interpreted in terms of this formalism and the results tabulated in publications such as the Steelmaking Data Sourcebook (1988). We used the method of Ma (2001) which employs the standard ε parameters, to ensure that the results obey the Gibbs–Duhem equation. Since most of the interaction parameters and infinite dilution activity coefficients (γ_i^o) were obtained at temperatures close to 1873 K, we extrapolated them to higher temperatures in the normal way:

$$\begin{aligned} \log \gamma_i^o(T) &= \frac{T^\circ}{T} \log \gamma_i^o(T^\circ) \\ \varepsilon_i^j(T) &= \frac{T^\circ}{T} \varepsilon_i^j(T^\circ) \end{aligned} \tag{5}$$

where T is the temperature of interest and T °C is the temperature at which the tabulated values apply.

2.2. Equilibrium constant and partition coefficient

Following Wade and Wood (2005) we consider partitioning as an exchange reaction involving Fe, FeO and the oxidized and reduced components of element M (reaction 3) :

$$\underset{\text{silicate}}{MO_{n/2}} + \frac{n}{2}\underset{\text{metal}}{Fe} = \frac{n}{2}\underset{\text{silicate}}{FeO} + \underset{\text{metal}}{M}$$

The equilibrium constant for reaction (3) is defined in terms of activities of components a_i, their mole fractions x_i and activity coefficients γ_i as follows:

$$\begin{aligned} K_a &= \frac{\left(a_{FeO}^{sil}\right)^{n/2} \cdot \left(a_M^{met}\right)}{\left(a_{Fe}^{met}\right)^{n/2} \cdot \left(a_{MO_{n/2}}^{sil}\right)} \\ &= \left[\frac{\left(x_{FeO}^{sil}\right)^{n/2} \cdot \left(x_M^{met}\right)}{\left(x_{Fe}^{met}\right)^{n/2} \cdot \left(x_{MO_{n/2}}^{sil}\right)}\right] \cdot \frac{\left(\gamma_{FeO}^{sil}\right)^{n/2} \cdot \left(\gamma_M^{met}\right)}{\left(\gamma_{Fe}^{met}\right)^{n/2} \cdot \left(\gamma_{MO_{n/2}}^{sil}\right)} \end{aligned} \tag{6}$$

In Eq. (6) the term in square brackets (K_D) is what is measured experimentally, activity coefficients in the metal were obtained as discussed above which leaves those for the silicate as the principal unknowns. Taking logarithms and rearranging yields:

$$\begin{aligned} \log K_a = \log &\left[\frac{\left(x_{FeO}^{sil}\right)^{n/2} \cdot \left(x_M^{met}\right)}{\left(x_{Fe}^{met}\right)^{n/2} \cdot \left(x_{MO_{n/2}}^{sil}\right)}\right] + \log \frac{\left(\gamma_M^{met}\right)}{\left(\gamma_{Fe}^{met}\right)^{n/2}} \\ &+ \log \frac{\left(\gamma_{FeO}^{sil}\right)^{n/2}}{\left(\gamma_{MO_{n/2}}^{sil}\right)} \end{aligned} \tag{7}$$

For each experiment we evaluated the first two terms on the right hand side of Eq. (7) and made the assumptions discussed below to correct, where necessary, for the third term, the activity coefficient ratio in the silicate melt.

Before considering the results, it is relevant to consider the likely magnitudes of the effects of the different solutes on K_D. Fig. 1 shows the calculated effects of up to 8% of C, S and Si on the predicted partition coefficients for V, Cr and Nb as obtained from the Wagner ε formalism. As can be seen, C has a strong effect on all three elements, with <2% C changing K_D for Nb by up to a factor of 6. The effect of S is particularly strong on Cr while Si is clearly the least important of the three solutes. In view of the large effects of S and C and bearing in mind that the steelmaking data (Steelmaking Data Sourcebook, 1988) generally apply for low concentrations (<8% solute) we restricted our regressions to experimental results in which the metal contained less than 10% C, S or Si.

3. RESULTS

3.1. Niobium

For Nb, recent experimental data (Corgne et al., 2008) indicate that K_D depends strongly on the composition of the silicate melt. Corgne et al.'s data indicate a

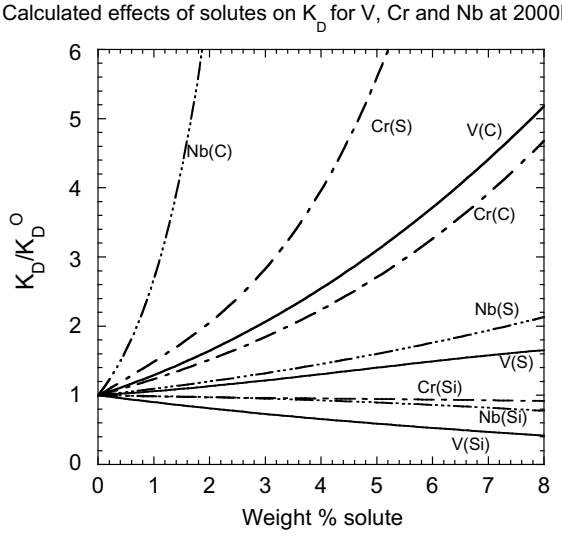

Fig. 1. Calculated effects of the major light solutes, C, S and Si on partition coefficients $K_D = \left[\frac{\left(x_{FeO}^{sil}\right)^{n/2} \cdot \left(x_M^{met}\right)}{\left(x_{Fe}^{met}\right)^{n/2} \cdot \left(x_{MO_{n/2}}^{sil}\right)}\right] \cong \frac{D_M}{D_{Fe}^{n/2}}$ (n is the valency of element M) for V, Nb and Cr at 2000 K. For ease of comparison all values are normalised to partition coefficients in pure Fe liquid.

correlation with the fraction of non-bridging oxygen atoms (N) in the silicate melt defined as follows:

$$\mathrm{N} = \frac{[2\mathrm{O} - 4T]}{T}$$

where, on a molar basis, O is the number of oxygen atoms and T is the number of tetrahedral cations (Si plus Al). Although the parameter N is a very crude description of the properties of silicate melts (O'Neill and Eggins, 2002) we adopt it here for lack of a better parameterisation.

In order to develop an expression to describe $\log K_D$ as a function of pressure, temperature and composition we must eliminate parameters which are already independently constrained. We therefore used thermodynamic data for pure end members (Barin et al., 1989) to fix the temperature dependence of partitioning. The reason for doing this is that very high-pressure experiments are normally conducted at higher temperatures than low-pressure experiments. Therefore if temperature and pressure terms are fitted to the data simultaneously they are strongly correlated with one another and extrapolations of the data become correspondingly uncertain. It is important , therefore to constrain the temperature term which is already well-known. However, if we do this, we need to introduce corrections for the solute in metal alloys, discussed above, and a term for activity coefficients in the silicate melt, which we have assumed to be a function of N. We thus expressed $\log K_D$ in the same manner as previously, except for the addition of a term involving N:

$$\log\left[K_D^{Nb}\right] + \log\frac{\left(\gamma_{Nb}^{met}\right)}{\left(\gamma_{Fe}^{met}\right)^{5/2}} = A + \frac{B}{T} + \frac{cP}{T} + \mathrm{d}N \qquad (8)$$

In Eq. (8) the B parameter is fixed by the thermodynamic data, 5 and 2 are the oxidation states of Nb and Fe respectively in the silicate, and K_D is the molar exchange coefficient, defined in Eq. (7), which approximates the weight value very closely, ie

$$K_D = \left|\frac{\left(x_{FeO}^{sil}\right)^{5/2}\cdot\left(x_{Nb}^{met}\right)}{\left(x_{Fe}^{met}\right)^{5/2}\cdot\left(x_{NbO_{5/2}}^{sil}\right)}\right| \approx \frac{D_{Nb}}{D_{Fe}^{5/2}}$$

For each experimental point we evaluated K_D and the activity coefficients of Nb and Fe in the metal phase and subtracted the B/T term. We then performed linear regression using Eq. (8).

$$\log\left[K_D^{Nb}\right] + \log\frac{\left(\gamma_{Nb}^{met}\right)}{\left(\gamma_{Fe}^{met}\right)^{5/2}} = 2.837 - \frac{13,240}{T} - \frac{114(\pm 43)P}{T} - 0.47(\pm 0.15)N \qquad (9)$$

We corrected all of our data points to an N value of 2.7, corresponding to peridotite mantle and plotted them in Fig. 2 as a function of reciprocal temperature. Corrected to N of 2.7, the final equation is:

$$\log\left[K_D^{Nb}\right] + \log\frac{\left(\gamma_{Nb}^{met}\right)}{\left(\gamma_{Fe}^{met}\right)^{5/2}} = 1.57 - \frac{13,240}{T} - \frac{114(\pm 43)P}{T} \pm 0.41 \qquad (10)$$

When used in core segregation scenarios, we assumed that, in liquid metal, γ_{Fe} is 1.0 (Raoult's Law) and γ_{Nb} (in the Henry's Law region) was obtained as follows from the Steelmaking Handbook (Steelmaking Data Sourcebook, 1988):

$$\log\gamma_{Nb}^{met} = \frac{-1310}{T}$$

Thus, the activity coefficient ratio can be eliminated by simply by transferring this term to the right hand side (see abstract).

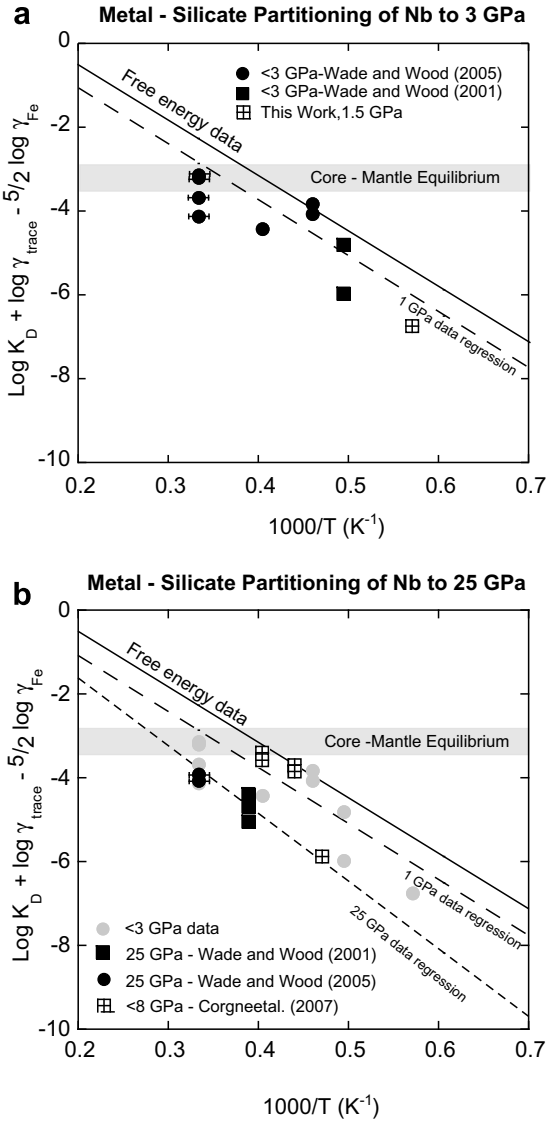

Fig. 2. The modified equilibrium constant for niobium $\log\left[K_D^{Nb}\right] + \log\left(\gamma_{Nb}^{met}\right) - \frac{5}{2}\log\left(\gamma_{Fe}^{met}\right)$ plotted as a function of 1000/T. Solid lines represent 1 bar free energy data (Barin et al., 1989) while dashed lines correspond to the best-fit equation at 1 and 25 GPa (see text). The horizontal grey field represents the values of equilibrium constant required to generate D_{Nb} values of 0.2–0.8, consistent with Table 1.

3.2. Vanadium

Wade and Wood (2005) assumed, following the observations of O'Neill and Eggins (2002), that there is no

dependence of K_D for vanadium on the composition of silicate melt. Making this assumption, which is strictly valid only for 2+ oxides, Wade and Wood found no significant dependence of V partitioning on pressure so that, within uncertainty, temperature and FeO/Fe ratio of the bulk material were considered to be the only important parameters. With the new data collected in this study we were able to re-examine these assumptions. First, we adopted the temperature dependence from the thermodynamic data and regressed for dependence on N and pressure. This gave:

$$\log\left[K_D^V\right] + \log\frac{\left(\gamma_V^{met}\right)}{\left(\gamma_{Fe}^{met}\right)^{3/2}} = 0.855 - \frac{8548}{T} - \frac{62(\pm 19)P}{T} - 0.101(\pm 0.029)N \quad (11)$$

One aspect of the result is encouraging in that the term depending on N (silicate melt composition) is much smaller than that for niobium, as might be expected because the charge on vanadium (+3) is much closer to that of Fe than is the charge on niobium (5+). We then corrected all of the data to a constant N value of 2.7 (peridotite) and plotted them as a function of reciprocal temperature in Fig. 3. For peridotitic compositions the final expression is:

$$\log\left[K_D^V\right] + \log\frac{\left(\gamma_V^{met}\right)}{\left(\gamma_{Fe}^{met}\right)^{3/2}} = 0.582 - \frac{8548}{T} - \frac{62(\pm 19)P}{T} \pm 0.08 \quad (12)$$

The results indicate that there is a small pressure effect on V partitioning which leads to an increase in the expected temperature of metal–silicate equilibration (Fig. 3) as the pressure increases. Application to core-formation scenarios relies on γ_{Fe} of 1.0 and γ_V given by (Steelmaking Data Sourcebook, 1988):

$$\log \gamma_V^{met} = \frac{-2055}{T}$$

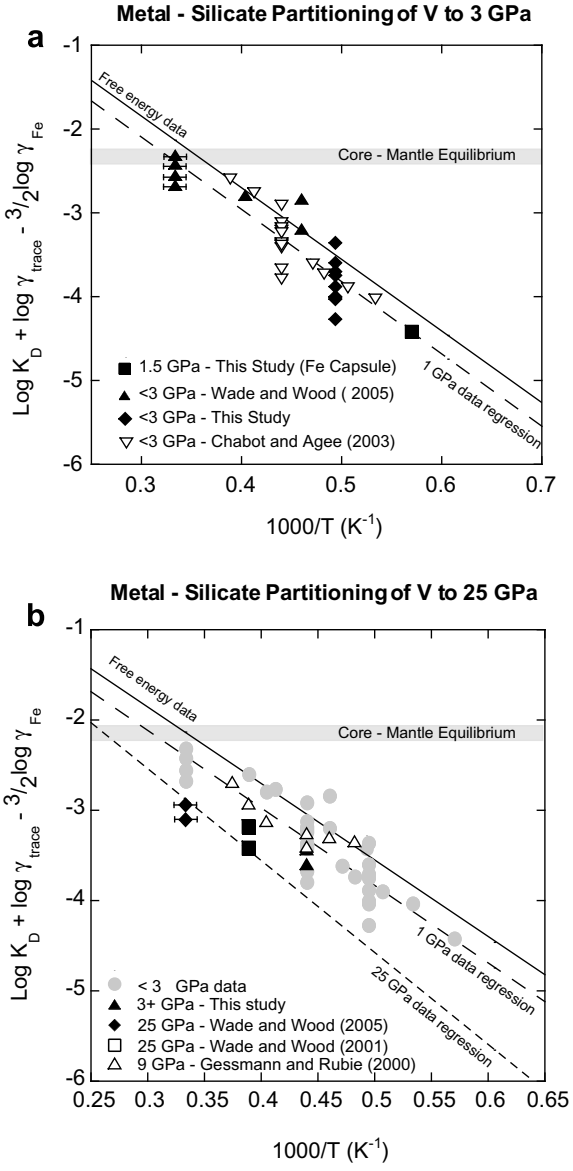

Fig. 3. The modified equilibrium constant for vanadium $\log\left[K_D^V\right] + \log\left(\gamma_V^{met}\right) - \frac{3}{2}\log\left(\gamma_{Fe}^{met}\right)$ plotted as a function of 1000/T with experimental data from this and previous studies. Solid lines represent 1 bar free energy data (Barin et al., 1989) while dashed lines correspond to the best-fit equation at 1 and 25 GPa (see text). The horizontal grey field represents the values of equilibrium constant required to generate D_V values of 1.5–2.2, consistent with Table 1. Note that points are shifted slightly relative to the figure in Wade and Wood (2005) because they have been corrected to NBO/T of 2.7 (see text).

3.3. Chromium

In the case of chromium there are a number of uncertainties and complications which do not apply in the cases of niobium and vanadium. Firstly, under conditions close to the iron–wüstite (IW) buffer there are large amounts of both Cr^{2+} and Cr^{3+} present in silicate melts (Berry and O'Neill, 2004) which makes it very difficult to treat the data using Eq. (7). Fortunately, metal-silicate partitioning experiments under conditions 2 or more log units below the IW buffer should be dominated by Cr^{2+} (Drake et al., 1989; Berry and O'Neill, 2004) so we have treated the data as if Cr^{2+} were the sole species present. A second problem is that there are no thermodynamic data for solid or liquid CrO available, so we are not able to constrain the temperature dependence of the equilibrium constant for the Fe–Cr exchange reaction. Therefore, we began by treating all parameters as unknown and fitted the data to:

$$\log\left[K_D^{Cr}\right] + \log\frac{\left(\gamma_{Cr}^{met}\right)}{\left(\gamma_{Fe}^{met}\right)} = A + \frac{B}{T} + \frac{cP}{T} + dN$$

We find, however, applying the F-test, that the N term is not significant. This is what would be expected from the results of O'Neill and Eggins (2002) who found that 2+ ions (in this case Fe^{2+} and Cr^{2+}) have essentially fixed activity ratio in silicate melts. Removing the N term and using multiple linear regression we obtained (Fig. 4):

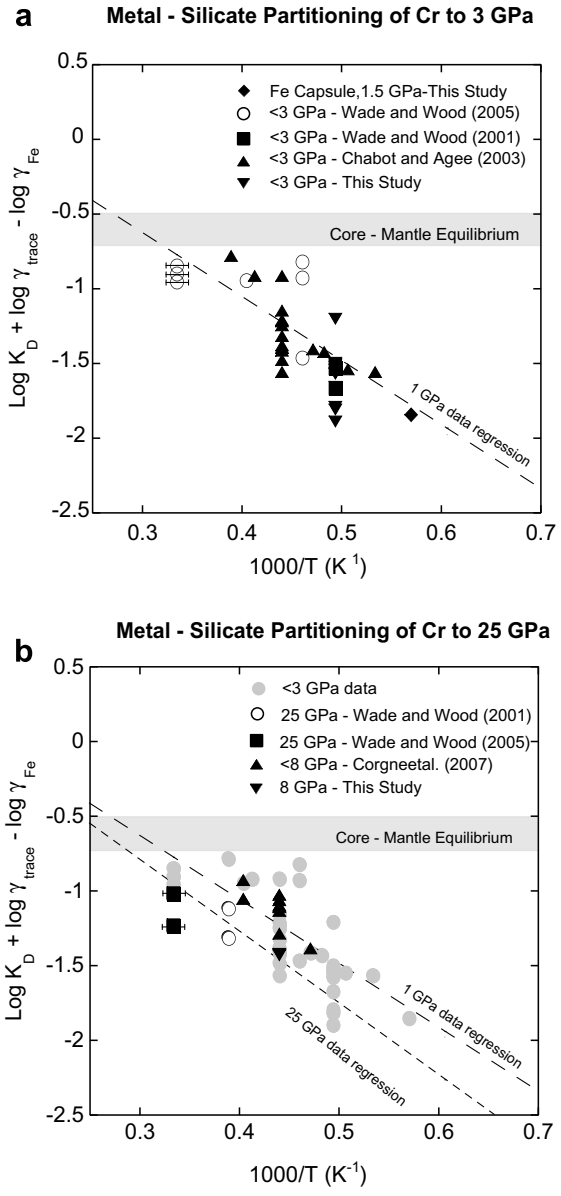

Fig. 4. The modified equilibrium constant for chromium $\log\left[K_D^{Cr}\right] + \log\left(\gamma_{Cr}^{met}\right) - \log\left(\gamma_{Fe}^{met}\right)$ plotted as a function of 1000/T with experimental data from this and previous studies. Dashed lines correspond to the best-fit equation at 1 and 25 GPa (see text). The horizontal grey field represents the values of equilibrium constant required to generate D_{Cr} values of 2.9–3.5 which is consistent with Table 1, if we assume that Cr is present in the Earth in chondritic ratio to refractory elements.

$$\log\left[K_D^{Cr}\right] + \log\frac{\left(\gamma_{Cr}^{met}\right)}{\left(\gamma_{Fe}^{met}\right)} = 0.643 - \frac{4232(\pm 538)}{T} - \frac{22(\pm 13)P}{T} \quad (13)$$

In applying this to core formation we use the activity coefficients from the Steelmaking Handbook which are 1.0 for both Fe and Cr.

4. APPLICATION TO CORE FORMATION

Following Wade and Wood (2005) we constructed a model in which the earth was grown in 1% steps and the core segregated at the base of a homogeneous magma ocean. The depth to the base of the magma ocean was assumed to increase in fixed proportion to the radius of the growing planet, as shown in Fig. 5. At each step the added metal (32.3% of the added mass) was equilibrated with the total mass of the mantle and then separated to the core without undergoing further re-equilibration. It should be noted that variants on this model in which the metal was assumed to equilibrate with only a small fraction of the mantle led to broadly similar results. Partitioning at each step was calculated using Eqs. (9)–(13) for Nb, V and Cr, together with the results of Wade and Wood (2005) for Ni, Co and Si.

Wade and Wood (2005) concluded that the current vanadium concentration of the silicate Earth could only be reconciled with core–mantle partitioning at temperatures close to the silicate liquidus if the Earth became more oxidized, with higher oxidized Fe content of the mantle, as it grew. Otherwise, at fixed Fe content of the mantle, much higher temperatures would, with their partitioning data, be required. We began by examining this conclusion with the revised partitioning equation for V (above) and the new data for Nb and Cr. We fixed the oxidized Fe content of the mantle at the current value of 6.26% (McDonough and Sun, 1995) and grew the Earth as described above, with the depth of the magma ocean being controlled by the required partitioning for the most pressure-sensitive elements, Ni and Co given in Table 1. The peridotite liquidus temperature was taken from experimental data (Zerr et al., 1998; Tronnes and Frost, 2002) and parameterized by Wade and Wood (2005) as a linear function of pressure (in GPa):

$$T(\mathrm{K}) = 1973 + 28.57P \quad (14)$$

We find, as shown in Fig. 6, that calculated vanadium partitioning ($D_V = 0.2$) cannot, with fixed oxidized Fe content of the mantle, match the observed core–mantle value of D_V of 1.5–2.2 (Table 1). If, in order to take account of uncertainties, we increase both the A and C parameters for vanadium by 1 standard error (effectively a maximum error treatment) we obtain an overall D_V value of 0.37 while increase of both parameters by 2 standard errors yields D_V of 0.73, still well below the anticipated range of Table 1. For Nb and Cr, shown in Fig. 6, we find, adopting the best-fit parameters for Eqs. (10) and (13) D_{Nb} of 0.08 and D_{Cr} of 1.1, the latter being well below the anticipated range of Table 1. Chromium partitioning, D_{Cr} can, however, be brought into the required range provided we increase both the A and C parameters by more than 1 standard error. Finally, for this scenario, of fixed oxidation state of the growing Earth, the core would only contain about 0.6% Si (using the partitioning equation of Wade and Wood, 2005). This is inconsistent with recent Si isotopic measurements of the silicate Earth which indicate that the core contains significant Si, perhaps around 5% (Georg et al., 2007). The conclusion is that an accreting Earth of fixed oxidation state cannot come close to matching the observed V concentration of

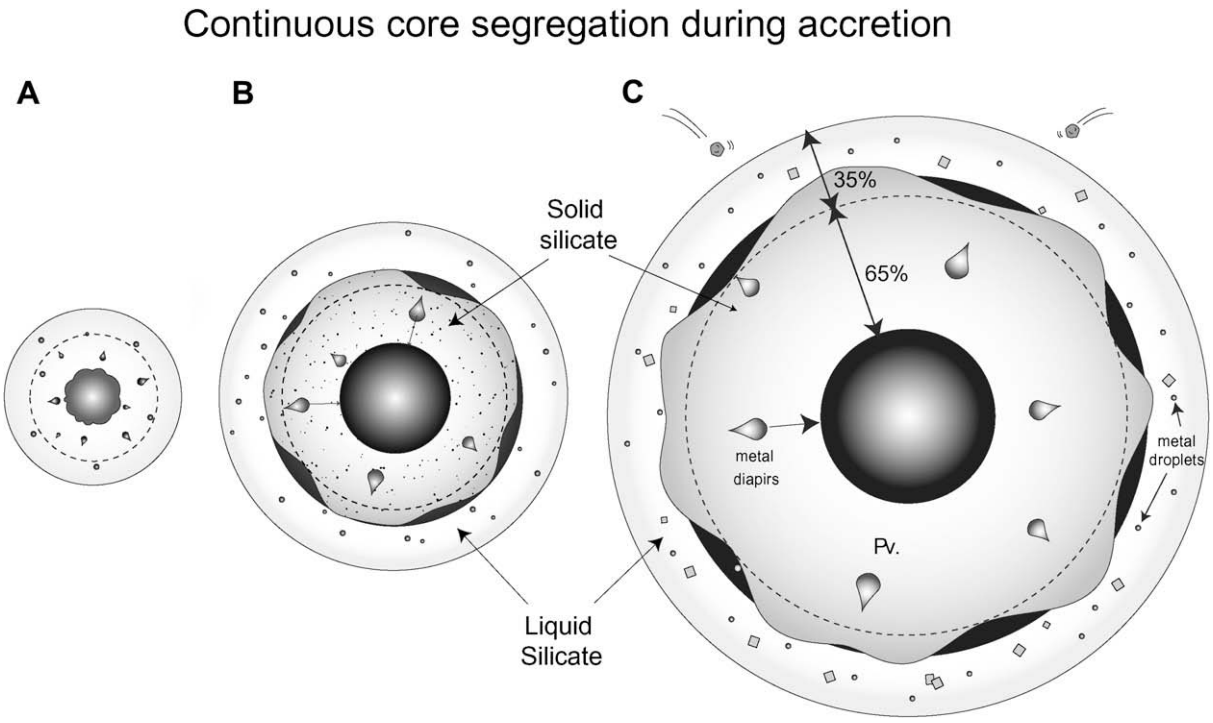

Fig. 5. Terrestrial growth model adopted in this study. As each increment is added to the earth, accreting metal is assumed to equilibrate completely with the mantle at a pressure corresponding to the base of the magma ocean. The metal is then isolated from the mantle and extracted to the core. For simplicity we assume a fixed depth ratio of upper (liquid) to lower solid mantle which, from partitioning of pressure-sensitive Ni corresponds to 35% of mantle depth.

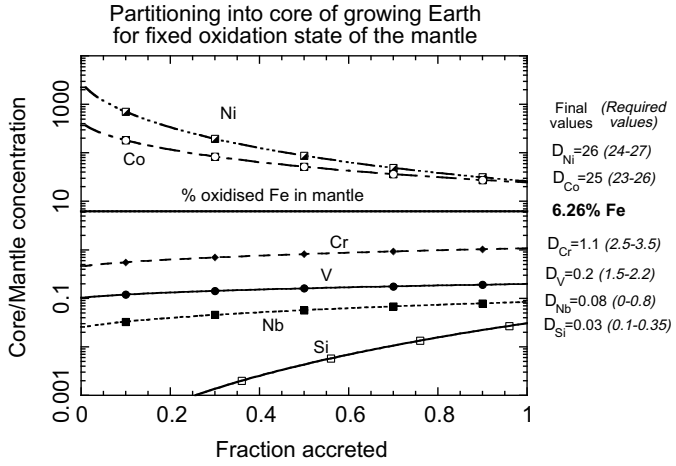

Fig. 6. Calculated partitioning into the core for an Earth with fixed oxidised Fe content of the mantle of 6.26%. The core was segregated as shown in Fig. 5 and the depth of the magma ocean fixed from Ni and Co partitioning (see text). In this scenario vanadium does not partition strongly enough into the core to match the observed mantle abundance, even, as discussed in the text by adopting maximum errors in the fit parameters.

the mantle unless temperatures are raised well above the silicate liquidus (as shown in Fig. 3), a similar conclusion to that of Chabot and Agee (2003). In order to bring core-mantle partitioning into agreement with values of Table 1, however, temperatures would need to be about 1200 °C above the liquidus, a result which seems physically unreasonable. Furthermore, Si and Nb partitioning are also extremely sensitive to temperature and such high temperatures would lead to D_{Nb} of ~3.8 (well above the possible range of Table 1) and to about 15% Si in the core, a value twice the most generous geochemical estimates (Allègre et al., 1995).

Following Wade and Wood (2005) we next investigated accretion under conditions of increasing oxidation state to

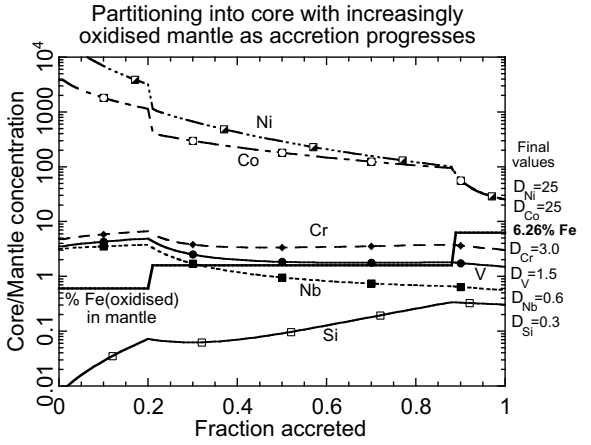

Fig. 7. Similar model to Fig. 6 except in this case the oxidised Fe content of the mantle increases from 0.6% to 6.26% in two steps at 0.2 and 0.89 of Earth accreted. The best fit values for V partitioning were adopted, and, as can be seen yield a final D_V which is consistent with the values of Table 1. Fit parameters for Nb, Cr and Si were adjusted within their uncertainties to yield D values consistent with Table 1.

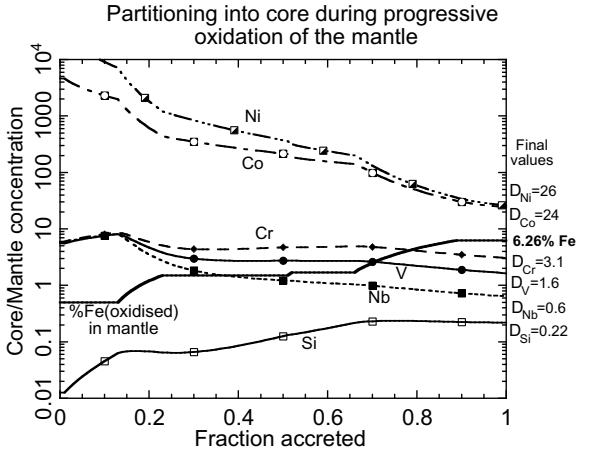

Fig. 8. Similar model to Fig. 7 except that the fit parameters for vanadium were adjusted by 1 standard error to yield maximum partitioning into the core (see text). For illustration, the required changes in oxidised Fe content of the mantle were spread out over extended periods of accretion and the conditions of accretion are, on average, slightly more oxidised than in Fig. 7. Vanadium partitioning is consistent with Table 1 as is partitioning for Nb, Cr and Si with minimal adjustments to the fit parameters (see text).

determine if this could, with our new data, generate partitioning behaviour consistent with Table 1. Fig. 7 shows results obtained by fixing the partitioning parameters for vanadium at the "best-fit" values given above. The maximum pressures and temperatures of equilibration reached at the base of the magma ocean were constrained from Ni and Co partitioning to be ~44 GPa and 3230 K, respectively. The average value of D_V can fit the 'required' range but only if the Earth becomes more oxidized during accretion. For illustrative purposes we allowed the mantle to oxidise in two steps at 20% and 89% accretion with the oxidized Fe content of the mantle increasing from 0.6% to 1.6% in the first and 1.6% to 6.26% in the second case. Nb, Si and Cr partitioning can also fit with observed values, provided some account is taken of the uncertainties in the fit-parameters. In the case of Nb, a final D_{Nb} of 0.6, consistent with Table 1, is obtained only if A and C parameters are pushed close to their minimum values (at the 1 standard error level). Otherwise, Nb is too strongly partitioned into the core. Cr and Si partitioning can, on the other hand, easily match the "required" values of Table 1 with only minimal adjustments to the fit parameters. In the example shown, the final Si content of the core would be 6.3%, in good agreement with the cosmochemical estimates of Allègre et al. (1995) and McDonough (2003). It should be emphasized that Fig. 7 is purely illustrative and that we are not proposing two large discontinuities in the oxidation state of the Earth. The purpose of the figure is to show that, in order to match the observed V contents of the silicate Earth, most of core segregation must have taken place under conditions more reducing than those implied by the current oxidized Fe content of the mantle. This progression from reduced to oxidized state is also consistent with partitioning of significant Si into the core, in agreement with the isotopic measurements of Georg et al. (2007).

Fig. 8 shows a similar accretion scenario to that of Fig. 7, but in this case the A and C fit-parameters for vanadium were both adjusted upwards by 1 standard error. This permits a final D_V within the required range with average conditions being slightly more oxidizing than those shown in Fig. 7. For illustration we have, in this case used more gradual increases in oxidation state than those shown in Fig. 7. The less reducing conditions enable D_{Nb} and D_{Cr} to match the expected values with parameters close to the best-fit values given above. The final D_{Si} value of 0.22 yields a Si content of the core of 4.6%, in good agreement with cosmochemical estimates and with the Si isotope data discussed above (Georg et al., 2007).

In summary, growth of the core in equilibrium with a mantle of current Fe content can only yield agreement with the observed mantle abundances of V if the temperature is ~1200 °C above the liquidus of mantle peridotite. Since segregation of the metal to the base of a magma ocean requires, if the magma ocean does not extend to the core-mantle boundary, that the temperature at the base be close to the silicate liquidus, such high temperatures are unlikely. Furthermore, they would lead to a Si content of the core of ~15% and D_{Nb} of about 3.8. Both these values are precluded by the concentrations of Si and Nb in the mantle and any plausible chondrite-like bulk composition of the Earth. If we make the more reasonable assumption that the base of the deepening magma ocean remains at temperatures of the peridotite liquidus, then the only possible solution requires the oxygen fugacity to have increased during accretion. In the simple scenario used here the magma ocean remained at about 35% of the depth of the mantle during accretion (Fig. 5). This gives a pressure rising to 44 GPa. The observed mantle depletions in the elements V, Ni, Co, Cr and Nb are reproduced provided the oxidized Fe content of the mantle increases from 0.5–1.0% up to 6.26

% during accretion. This is equivalent to an increase in oxygen fugacity of between 1.6 and 2.2 log units. Given this constraint core equilibration remains on the liquidus and the metal contains about 6% Si, in good agreement with cosmochemical estimates.

Oxidation of the Earth during accretion could have been the result of addition of progressively more oxidized materials as the young Earth grew. Internal mechanisms operating during core formation would also, however, have lead to increasing oxidation during accretion. Firstly, the core segregation conditions depicted in Figs 7 and 8 lead to several weight per cent of Si being transferred from silicate to metal. The oxygen released by this reduction of SiO_2 would most plausibly have oxidized metallic Fe and increased the FeO content of the mantle. Secondly, the Earth's lower mantle is currently about 80% by volume magnesium silicate perovskite $(Mg,Fe)SiO_3$ (Wood, 2000). This phase accommodates the 5% Al_2O_3 which it contains in peridotite compositions by a coupled substitution with Fe^{3+} (Wood and Rubie, 1996; McCammon, 1997) as follows:

$$Mg^{2+}Si^{4+} \leftrightarrow Fe^{3+}Al^{3+}$$

This substitution mechanism is so stable that it forces disproportionation of ferrous iron into ferric iron plus metal (Frost et al., 2004) by reactions such as:

$$3\underset{\text{Oxide}}{Fe^{2+}O} + \underset{\text{Garnet}}{Fe_3^{2+}Al_2Si_3O_{12}} = 2\underset{\text{Perovskite}}{Fe^{3+}AlO_3} + 3\underset{\text{Perovskite}}{Fe^{2+}SiO_3} + \underset{\text{Metal}}{Fe^0} \quad (15)$$

This means that, as perovskite began to crystallize from the magma ocean, it dissolved ferric iron as $FeAlO_3$ component and produced Fe metal. This process would have begun when perovskite was stabilised in the mantle corresponding to a growing Earth of about 11% of its current size. Wade and Wood (2005) argued that downward segregation of metal during growth of the core should have carried with it some of the metal produced by disproportionation. When combined with episodic release of Fe^{3+} from the perovskite layer by dissolution caused by impact-heating, the result would have been to increase the oxidized Fe content of the mantle.

5. CONCLUSIONS

Our new partitioning data for V, Cr and Nb, when added to data from the literature, enable additional constraints on estimates of the physical conditions of core segregation. We started with the assumptions that the metallic core segregated to the base of a magma ocean which did not extend to the core–mantle boundary (Li and Agee, 1996; Righter and Drake, 1997; Righter, 2003) and assumed that the core separated progressively as the Earth grew. Under these conditions the temperature and pressure at the base of the magma ocean would have increased along the silicate liquidus (or between liquidus and solidus) as the Earth grew. The maximum pressure at the base of the magma ocean was constrained by the observed core-mantle partitioning of Ni and Co (Table 1), which are very pressure-sensitive. We find, with such a model, that the current V content of the mantle cannot be reconciled with core segregation under conditions of fixed relative oxygen fugacity (corresponding to fixed FeO content of the mantle), even if 2 standard error uncertainties are applied to the fit-parameters. In this case, with maximum uncertainties applied, the prediction is that only 27% of the Earth's V is in the core, whereas mass balance based on the CI chondrite model indicates that the actual figure is 47%.

There are two simple ways of relaxing the model so that the V partitioning results become consistent with Table 1. The first is to allow temperature to increase above the silicate liquidus. Although such a departure is physically unreasonable, it is possible to achieve the appropriate partitioning values for V if temperatures are raised to about 1200 °C above the liquidus. The result, however, would be a core containing about 15% Si and >60% of the Earth's niobium, figures several times the plausible amounts (Allegre et al., 1995) (Table 1). A more likely scenario is that the Earth was initially very reduced and became more oxidized as it accreted (Wänke, 1981; Wänke and Dreibus, 1988; O'Neill, 1991). In this case we find that, with temperatures fixed on the silicate liquidus, the V, Cr and Nb contents of core and mantle are easily matched to those calculated from the chondritic abundances of refractory elements in the Earth. From Ni partitioning, the magma ocean is calculated to maintain a thickness approximately 35% of the depth to the core-mantle boundary in the accreting Earth. Increasing oxidation requires the oxidized Fe content of the mantle to increase from 0.5–1.0% to the current value of 6.26% as the Earth grew. This model also reproduces the calculated core-mantle partitioning of Ni and Co and yields a Si content of the core of approximately 6%, in good agreement with cosmochemical estimates.

ACKNOWLEDGMENTS

This work commenced at the University of Bristol with support from NERC Grant GR3/11535 and continued at Macquarie University with support from ARC Grants FF0456999 and DP0664537. This study used instrumentation funded by ARC LIEF and DEST Systemic Infrastructure Grants, Macquarie University and industry. Nancy Chabot and Elizabeth Cottrell are thanked for their reviews. We also thank Stuart Kearns for assistance with the microprobe analyses.

REFERENCES

Allègre C. J., Poirier J.-P., Humler E. and Hofmann A. W. (1995) The chemical composition of the Earth. *Earth Planet. Sci. Lett.* **134**(3–4), 515–526.

Barin I., Sauert F., Schultze-Rhonhof E. and Sheng W.S. (1989) *Thermochemical data of pure substances, Part I and Part II*, CH Verlagsgesellschaft.

Berry A. J. and O'Neill H. S. (2004) A XANES determination of the oxidation state of chromium in silicate glasses. *Am. Miner.* **89**, 790–798.

Canup R. M. (2004) Origin of terrestrial planets and the Earth–Moon system. *Phys. Today* **57**(4), 56–62.

Chabot N. L. and Agee C. B. (2003) Core formation in the Earth and Moon: new experimental constraints from V, Cr, and Mn. *Geochim. Cosmochim. Acta* **67**(11), 2077–2091.

Corgne A., Keshav S., Wood B. J., McDonough W. F. and Fei Y. (2008) Metal–silicate partitioning and constraints on core

composition and oxygen fugacity during Earth accretion. *Geochim. Cosmochim. Acta* **72**, 574–589.

Drake M. J., Newsom H. E. and Capobianco C. J. (1989) V, Cr, and Mn in the Earth, Moon, Epb, and Spb and the origin of the Moon—experimental studies. *Geochim. Cosmochim. Acta* **53**(8), 2101–2111.

Frost D. J., Liebske C., Langenhorst F., McCammon C. A., Trønnes R. G. and Rubie D. C. (2004) Experimental evidence for the existence of iron-rich metal in the Earth's lower mantle. *Nature* **428**(6981), 409–412.

Georg R. B., Halliday A. N., Schauble E. A. and Reynolds B. C. (2007) Silicon in the Earth's core. *Nature* **447**, 1102–1106.

Gessmann C. K. and Rubie D. C. (2000) The origin of the depletions of V, Cr and Mn in the mantles of the Earth and Moon. *Earth Planet. Sci. Lett.* **184**(1), 95–107.

Gessmann C. K., Wood B. J., Rubie D. C. and Kilburn M. R. (2001) Solubility of silicon in liquid metal at high pressure: implications for the composition of the Earth's core. *Earth Planet. Sci. Lett.* **184**(2), 367–376.

Halliday A. N. (2004) Mixing, volatile loss and compositional change during impact- driven accretion of the Earth. *Nature* **427**(6974), 505–509.

Kilburn M. R. and Wood B. J. (1997) Metal–silicate partitioning and the incompatibility of S and Si during core formation. *Earth Planet. Sci. Lett.* **152**(1–4), 139–148.

Kleine T., Munker C., Mezger K. and Palme H. (2002) Rapid accretion and early core formation on asteroids and the terrestrial planets from Hf–W chronometry. *Nature* **418**(6901), 952–955.

Kleine T., Mezger K., Palme H. and Munker C. (2004) The W isotope evolution of the bulk silicate Earth: constraints on the timing and mechanisms of core formation and accretion. *Earth Planet. Sci. Lett.* **228**(1–2), 109–123.

Li J. and Agee C. B. (1996) Geochemistry of mantle–core differentiation at high pressure. *Nature* **381**, 686–689.

Li J. and Agee C. B. (2001) The effect of pressure, temperature, oxygen fugacity and composition on partitioning of nickel and cobalt between liquid Fe–Ni–S alloy and liquid silicate: implications for the Earth's core formation. *Geochim. Cosmochim. Acta* **65**(11), 1821–1832.

Ma Z. T. (2001) Thermodynamic description for concentrated metallic solutions using interaction parameters. *Metall. Mater. Trans. B-Process Metall. Mater. Process. Sci.* **32**(1), 87–103.

McCammon C. (1997) Perovskite as a possible sink for ferric iron in the lower mantle. *Nature* **387**(6634), 694–696.

McDonough W. F. (2003) Compositional model for the Earth's core. In *Treatise on Geochemistry*, v. 2 (ed. R. W. Carlson). Elsevier-Pergamon, Oxford, pp. 547–568.

McDonough W. F. and Sun S.-S. (1995) The composition of the Earth. *Chem. Geol.* **120**(3–4), 223–253.

Norman M., Garcia M. O. and Pietruszka A. J. (2005) Trace-element distribution coefficients for pyroxenes, plagioclase, and olivine in evolved tholefites from the 1955 eruption of Kilauea Volcano, Hawaii, and petrogenesis of differentiated rift-zone lavas. *Am. Miner.* **90**(5–6), 888–899.

O'Neill H. S. C. (1991) The origin of the Moon and the early history of the Earth—a chemical model. 2. The Earth. *Geochim. Cosmochim. Acta* **55**(4), 1159–1172.

O'Neill H. S. C. and Eggins S. M. (2002) The effect of melt composition on trace element partitioning: an experimental investigation of the activity coefficients of FeO, NiO, CoO, MoO_2 and MoO_3 in silicate melts. *Chem. Geol.* **186**(1–2), 151–181.

Righter K. (2003) Metal–silicate partitioning of siderophile elements and coreformation in the early Earth. *Annu. Rev. Earth Planet. Sci.* **31**, 135–174.

Righter K. and Drake M. J. (1997) Metal–silicate equilibrium in a homogeneously accreting earth: new results for Re. *Earth Planet. Sci. Lett.* **146**(3–4), 541–553.

Rubie D. C., Melosh H. J., Reid J. E., Liebske C. and Righter K. (2003) Mechanisms of metal–silicate equilibration in the terrestrial magma ocean. *Earth Planet. Sci. Lett.* **205**(3–4), 239–255.

Rudnick R. L., Barth M., Horn I. and McDonough W. F. (2000) Rutile-bearing refractory eclogites: missing link between continents and depleted mantle. *Science* **287**(5451), 278–281.

The Japan Society for the Promotion of Science (1988) *Steelmaking Data Sourcebook*. Gordon and Breach, New York.

Thibault Y. and Walter M. J. (1995) The influence of pressure and temperature on the metal–silicate partition coefficients of nickel and cobalt in a model C1 chondrite and implications for metal segregation in a deep magma ocean. *Geochim. Cosmochim. Acta* **59**(5), 991.

Tronnes R. G. and Frost D. J. (2002) Peridotite melting and mineral-melt partitioning of major and minor elements at 22–24.5 GPa. *Earth Planet. Sci. Lett.* **197**(1–2), 117–131.

Wade J. and Wood B. J. (2001) The Earth's 'missing' niobium may be in the core. *Nature* **409**(6816), 75–78.

Wade J. and Wood B. J. (2005) Core formation and the oxidation state of the Earth. *Earth Planet. Sci. Lett.* **236**, 78–95.

Wagner C. (1962) *Thermodynamics of Alloys*. Addison-Wesley, Reading, MA.

Walker D., Carpenter M. A. and Hitch C. M. (1990) Some simplifications to multianvil devices for high pressure experiments. *Am. Miner.* **75**, 1020–1028.

Wänke H. (1981) Constitution of the terrestrial planets. *Philos. Trans. Roy. Soc. Lond.* **A303**, 287–302.

Wänke H. and Dreibus G. (1988) Chemical-composition and accretion history of terrestrial planets. *Philos. Trans. Roy. Soc. Lond. A-Math. Phys. Eng. Sci.* **325**(1587), 545–557.

Wood B. J. (2000) Phase transformations and partitioning relations in peridotite under lower mantle conditions. *Earth Planet. Sci. Lett.* **174**(3–4), 341–354.

Wood B. J. and Rubie D. C. (1996) The effect of alumina on phase transformations at the 660-kilometer discontinuity from Fe–Mg partitioning experiments. *Science* **273**, 1522–1524.

Yin Q. Z., Jacobsen S. B., Yamashita K., Blichert-Toft J., Telouk P. and Albarede F. (2002) A short timescale for terrestrial planet formation from Hf–W chronometry of meteorites. *Nature* **418**(6901), 949–952.

Zerr A., Diegeler A. and Boehler R. (1998) Solidus of Earth's deep mantle. *Science* **281**, 243–246.

Associate editor: F.J. Ryerson